JOURNAL OF MATERIALS SCIENCE 32 (1997) 6221–6225

An algorithm to optimize the equivalent network for dielectrics

S. N. AL-REFAIE
Department of Electronic Engineering, Faculty of Applied Engineering, Yarmouk University, Irbid, Jordan

An algorithm is derived to optimize the number of branches in the equivalent network representing dielectric dispersion with many relaxation times. The algorithm is characterized by deriving general normalized relations. Satisfactory results are obtained for a network with more than 50% reduction in the number of branches for dispersion data of perfluoropolyether dielectric. The method is directly applicable to dispersion relations featuring weakly overlapping arcs in the complex plane of the dielectric constant. The procedure is also extendible for relations with strong arcs overlapping, such as in polymers and composite materials.

1. Introduction

Most dielectric materials employed in technological and industrial applications have dispersion with frequency featuring many relaxation times. In those materials the dispersion of dielectric constant is characterized by a continuum in relaxation time rather than discrete time constants. Subsequently their equivalent networks take distributed forms. However, practical applications require implementing these networks as parts of the models used in industrial and electronic systems. Therefore, a distributed network has to be reduced to a discrete form constituting lumped elements. This has been realized for dielectrics of ZnO and InP-oxide in the frequency range of few tens of Hz to several MHz [1, 2]. Evaluation of the networks have been facilitated using the relaxation time distributions (RTD), as derived from the multiple-arc analysis, along with their pertinent parametric functions [3]. In the adopted procedure, the discrete elements were determined over equal intervals of the relaxation time function. The accuracy of the network was then examined by comparing the experimentally evaluated components of the complex dielectric constant with those computed from the discrete equivalent network. However, practicality of the model dictates also that the network should be simple. This can be accomplished by reducing the number of branches, but at the expense of accuracy. Alternatively, this paper suggests a novel approach to optimize the network while preserving a high degree of controllable accuracy. The devised algorithm is based on the RTD function and its derivative.

2. Basic formulations

In principle, the proposed approach is equally applicable to dispersion relations describing single circular arc or multiple arcs in the complex plane of the dielectric constant. Meanwhile, to grasp the essential characteristics of the approach, a single arc relation is considered in the analysis.

For a dielectric dispersion featuring single arc relation in the complex plane, the real and imaginary components of the constant are, respectively, expressed as [4]

$$\varepsilon'(\omega) = \varepsilon_\infty + (\varepsilon_s - \varepsilon_\infty)\int_{-\infty}^{\infty} \frac{f(u)}{1+\omega^2\tau^2}\,du \quad (1)$$

and

$$\varepsilon''(\omega) = (\varepsilon_s - \varepsilon_\infty)\int_{-\infty}^{\infty} \frac{\tau\omega f(u)}{1+\omega^2\tau^2}\,du \quad (2)$$

where $f(u)$ is the relaxation time distribution and given as [5]

$$f(u) = \frac{1}{2\pi}\frac{\sin(\alpha\pi)}{\cosh[(1-\alpha)u] - \cos(\alpha\pi)} \quad (3)$$

with u as the relaxation time, and τ, the function

$$u = \ln(\tau/\tau_0)$$

ε_s and ε_∞ are the static and high frequency constants, respectively. τ_0 is the most probable relaxation time and α designates the degree of spread in the distribution taking values between 0 and 1, with the 0 value corresponding to single relaxation time [5]. Equations 1 and 2 lead to a direct network representation for the dielectric in the form of a distributed R-C (Resistance-Capacitance) network, as shown in Fig. 1. The corresponding network elements are expressed as [4]

$$\delta\varepsilon = \bar{\varepsilon}(u)du$$

and

$$\delta\sigma = \bar{\sigma}(u)du$$

where $\bar{\varepsilon}(u)$ and $\bar{\sigma}(u)$ are parametric variables given as [3]

$$\bar{\varepsilon}(u) = (\varepsilon_s - \varepsilon_\infty)f(u) \quad (4)$$

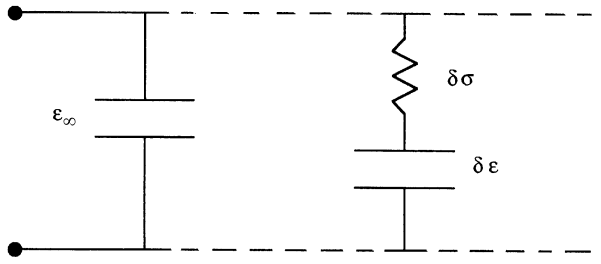

Figure 1 The distributed R-C equivalent network.

and

$$\bar{\sigma}(u) = \varepsilon_0 \bar{\varepsilon}(u)/\tau \tag{5}$$

The parametric functions can provide a consistent and solid means to derive the discrete network, namely by integrating Equations 4 and 5 over a constant interval Δu whereby an R-C branch is defined. The procedure is then repeated over the effective u-range. The total permittivity is subsequently obtained as

$$\varepsilon'(\omega) \cong \varepsilon_\infty + \sum_{K=1}^{L} \frac{(\varepsilon_s - \varepsilon_\infty)\int f(u)\mathrm{d}u|_{\Delta u}}{1 + \omega^2 \tau_K^2} \tag{6}$$

where K designates a branch, and L is the number of branches over the effective u-range. Referring to Equations 4 and 5, τ_K is given as

$$\tau_K = \frac{\tau_0 \int f(u)\mathrm{d}u|_{\Delta u}}{\int f(u)\mathrm{e}^{-u}\mathrm{d}u|_{\Delta u}} \tag{7}$$

for the K branch.

It is worth pointing out that in the limit where Δu tends to zero, Equation 6 approaches Equation 1. A similar approach has been applied on the dispersion data of ZnO varistor and InP-oxide yielding, respectively, 20 and 8 branches. With the resulting networks, satisfactory degrees of accuracy have been realized over the frequency range of 30 Hz to nearly 10 MHz [1, 2].

However, such an arbitrary procedure may, unnecessarily, yield a large number of branches because it relates the accuracy of the network to the number of branches only. Alternatively, a new method is devised here whereby the number of branches is functionally related to the RTD function and its derivative. The proposed procedure is merely concerned with the integration processing of Equation 4, over the interval Δu. Keeping Δu constant throughout the entire u-range is considered as a linear processing. Hence, the task here is to devise a non-linear processing whereby the interval Δu becomes variable. To derive this trend of variation, exact differential treatment is regarded more appropriate. Subsequently, Δu is initially replaced by a small incremental quantity δu. As the integral of Equation 4 represents the area under $\bar{\varepsilon}(u)$, shown in Fig. 2 then comparing the incremental areas δA_2 and δA_1, at arbitrary u-value, yields

$$\frac{\delta A_2}{\delta A_1} = \frac{\delta f(u)\delta u}{2 f(u)\delta u} \tag{8}$$

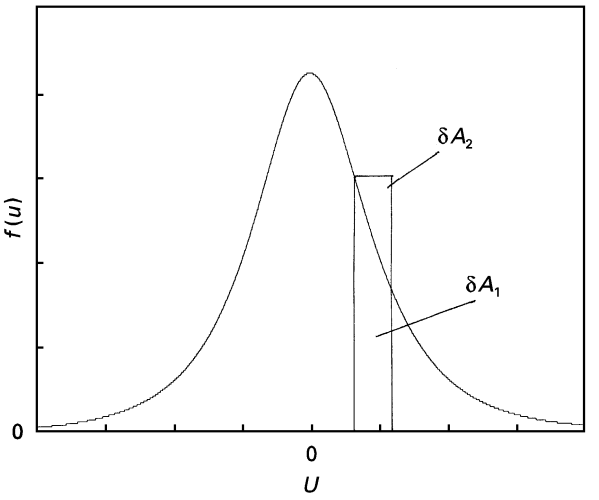

Figure 2 The incremental areas under a distribution function $f(u)$.

As the increments used tend to zero in the limit, they are replaced by differential notation. The numerator in Equation 8 is regarded as a second order differential, while the denominator designates a first order differential. Hence, the ratio in Equation 8 can be equated to a new differential ∂z. By assuming ∂z as an infinitesimal independent quantity, then the following relation is established

$$\frac{\partial f(u)}{f(u)} = \partial z$$

the factor of 2 being merged with ∂z. Substituting $\partial f(u)$ by $\bar{f}(u)\partial u$, where $\bar{f}(u) = \partial f(u)/\partial u$, and taking into account a possible negative value for $\bar{f}(u)$, then

$$\partial u = \left|\frac{f(u)}{\bar{f}(u)}\right| \partial z \tag{9}$$

Although, ∂u can, in principle, be expressed in terms of any variable coefficient with ∂z, the derived function has certain desirable particulars. On one hand, the coefficient is correlated to the distribution function, and further resembles the distribution even symmetry around u. On the other hand, the coefficient introduces no substantial error under the condition of a high $f(u)$ and low $\bar{f}(u)$ values, where Δu interval takes a large value. As indicated by Equation 3 the interval coefficient in Equation 9 is strongly influenced by the spread parameter α. Subsequently, the relevant characteristics are investigated in the next section.

3. Method characterization

Substituting $f(u)$ and $\bar{f}(u)$ the interval coefficient in Equation 9 becomes

$$\left|\frac{f(u)}{\bar{f}(u)}\right| = (1-\alpha)^{-1}\,|\coth(1-\alpha)u - \cos(\alpha\pi)\,\mathrm{csch}(1-\alpha)u| \tag{10}$$

where (csch = hyperbolic cosecant). Fig. 3 depicts the variations of the interval coefficient with u for

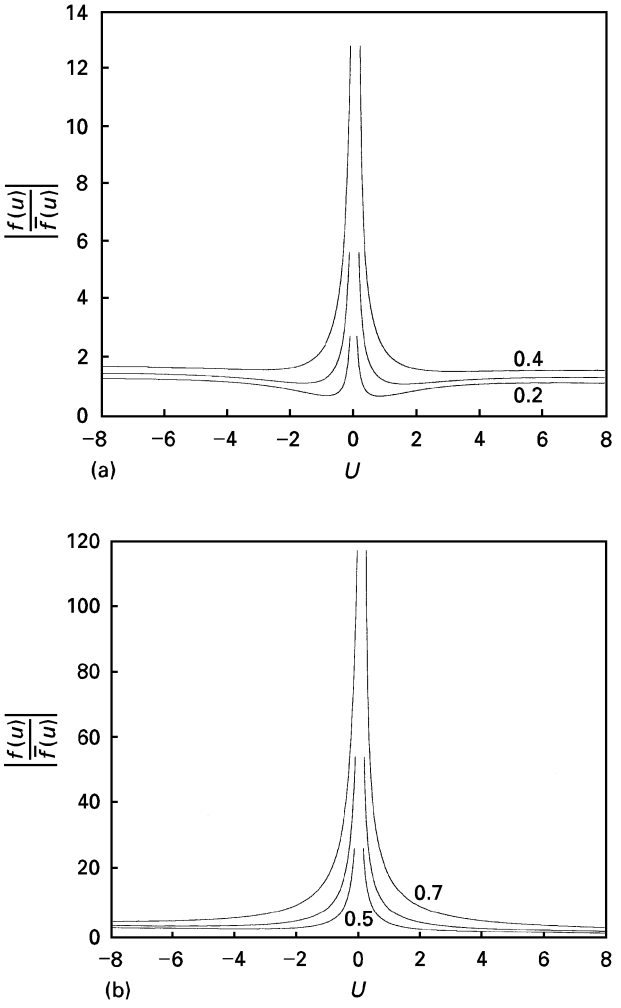

Figure 3 (a) The interval coefficient characteristics with u for the α range of 0.2–0.4. (b) The interval coefficient characteristics with u for the α range of 0.5–0.7.

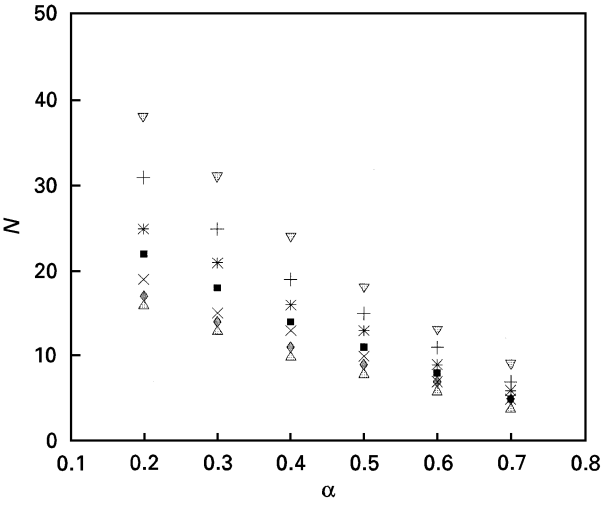

Figure 4 The variation of number of branches N with the spread parameter α for different Δz values: (▽) 0.4; (+) 0.5; (∗) 0.6; (■) 0.7; (×) 0.8; (◆) 0.9; (△) 1.0.

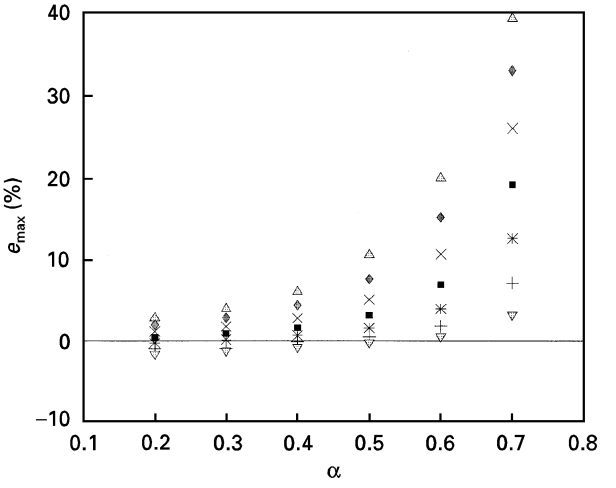

Figure 5 The variation of e_{max} with α for different Δz values: (▽) 0.4; (+) 0.5; (∗) 0.6; (■) 0.7; (×) 0.8; (◆) 0.9; (△) 1.0.

different values of α ranging from 0.2 to 0.7. Consequently, the α parameter has a direct influence on the number of network branches. This aspect is further characterized by assigning the value of 16 for the u-range. This corresponds to more than eight orders of magnitude from the upper to the lower frequency. The upper frequency ω_h is taken at τ_1^{-1} and normalized to τ_0^{-1}. τ_1^{-1} marks the lower limit in the u-range. In the course of approximation whereby Δu and Δz replace ∂u and ∂z, Δz is designated as the accuracy parameter for the discrete network. Fig. 4 illustrates a group of characteristics relating the number of branches N to the spread parameter α for different values of Δz. To insure a high degree of computational accuracy, the effective u-range is divided into 1600 segments. This measure seems to be necessary since Equation 10 takes very high values near $u = 0$. Furthermore, following the symmetry in Equation 10, Δu intervals are evaluated symmetrically over the u-range so that equal intervals are located at equal positions from $u = 0$.

Close examination of Equation 1 in conjunction with Equation 6 indicates that maximum percentage of error, e_{max}, occurs at high frequency. This feature is based on discarding ε_∞ from Equations 1 and 6, i.e. regarding only the dispersive parts in the expressions. Under this condition, e_{max} takes the form

$$e_{max} = 1 - \frac{\sum_{K=1}^{N} \frac{\int f(u)\mathrm{d}u|_{\Delta u}}{(1+\omega_h^2\tau_k^2)}}{\left(\int_{-\infty}^{\infty} \frac{f(u)}{(1+\omega_h^2\tau^2)}\mathrm{d}u\right)} \qquad (11)$$

Fig. 5 shows the variation of e_{max} with α for different values of the accuracy factor Δz. The very small negative error values at low α values can be attributed to the inevitable error in numerical computation. These characteristics can be directly employed in the design of equivalent network for dielectrics, provided that the dispersion data fits circular arc, or arcs, in the complex plane of the dielectric constant. The procedure of optimization is demonstrated on the dispersion data for perfluoropolyether dielectric and given in the next section.

4. Results and discussion

The dispersion data reported for perfluoropolyether dielectric [6] describes a single circular arc over the

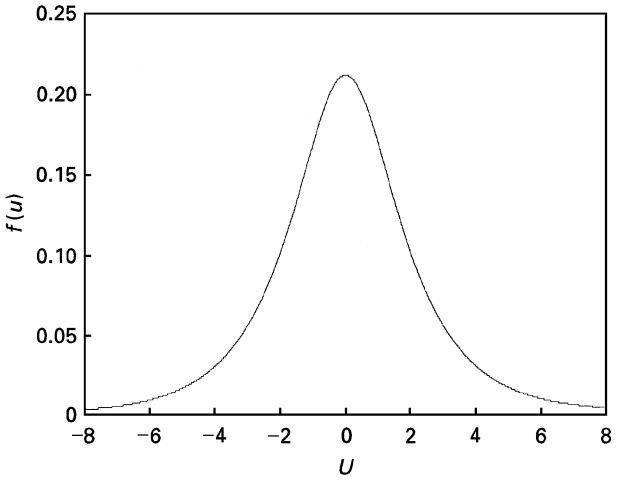

Figure 6 The RTD function for perfluoropolyether dielectric.

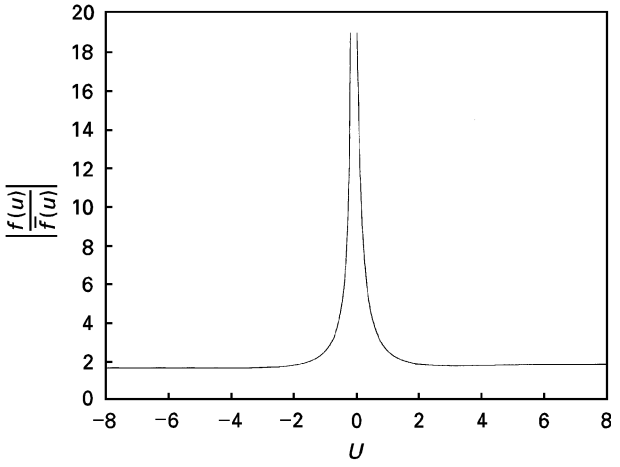

Figure 7 The interval coefficient variation with u for the perfluoropolyether dielectric.

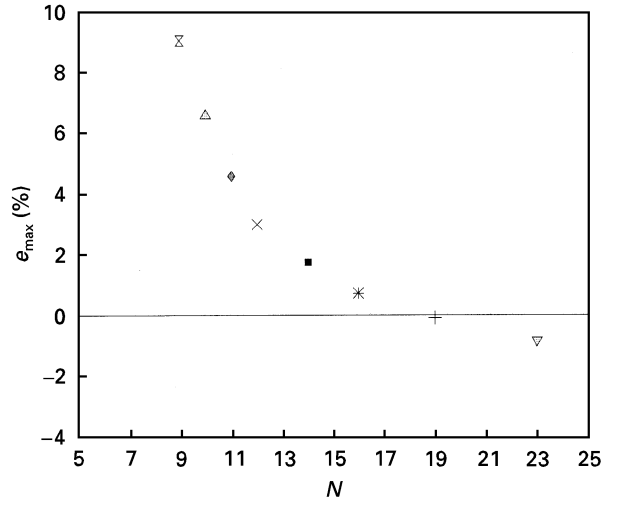

Figure 8 The variation of e_{max} with N for perfluoropolyether dielectric for different Δz values: (▽) 0.4; (+) 0.5; (∗) 0.6; (■) 0.7; (×) 0.8; (◆) 0.9; (△) 1.0; (▽) 1.1.

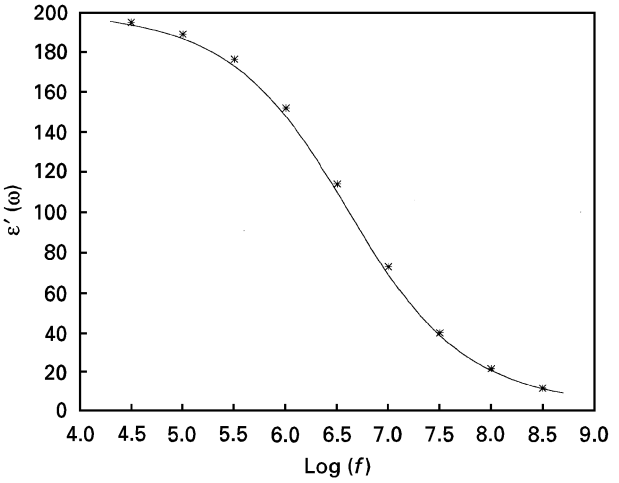

Figure 9 The variation of relative permittivity with frequency for distributed and discrete networks. (——) Distributed network (exact); (∗) discrete network (approximate).

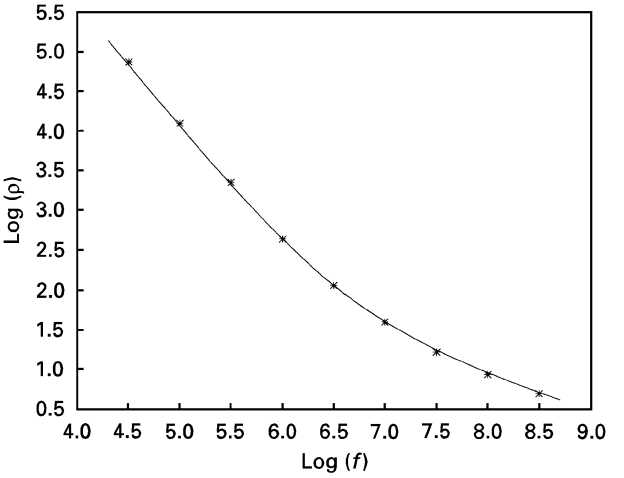

Figure 10 The variation of resistivity with frequency for distributed and discrete networks. (——) Distributed network (exact); (∗) discrete network (approximate).

frequency range of 100 kHz to 100 MHz. The evaluated parameters of the arc are [2] $\varepsilon_s = 202$, $\varepsilon_\infty = 3$, $\alpha = 0.41$, $\tau_0 = 40 \times 10^{-9}$ s. Using the procedure and relations outlined in Section 3, a complete characterization for the optimum network has been achieved. The RTD function is shown in Fig. 6, while the interval factor, given by Equation 10, is depicted in Fig. 7. Correlation of the error e_{max} to the number of branches N is illustrated in Fig. 8 for a range of values for the accuracy factor Δz, indicating an expected trend of variation. However, the small negative e_{max} value at a high N value could again be attributed to the inevitable error in numerical computation.

To verify the effectiveness of this methodology, the point corresponding to minimum number of branches, in Fig. 8, is chosen with $N = 9$ and $e_{max} = 9.0\%$. Subsequently, exact distributed network is compared with the nine branches network in Fig. 9 for $\varepsilon'(\omega)$ and in Fig. 10 for the resistivity $\rho(\omega)$. Computations of these variables have been carried out using Equations 1, 2, 6, 9, 10 and 11. Both figures indicate satisfactory agreements over the frequency range from 50 kHz to 100 MHz, which is close to that specified by the u-range. This achievement marks more than 50% reduction of branches when compared to an earlier reported network of 20 branches [2], in addition to an improved accuracy. The network parameters are given in Table I.

TABLE I Network parameters

Branch K	τ_K (s)	ε_K (relative)	σ_K $(\Omega\,\mathrm{cm})^{-1}$
1	3.489×10^{-11}	1.85	4.69×10^{-1}
2	2.201×10^{-10}	5.50	2.21×10^{-1}
3	1.354×10^{-9}	16.35	1.07×10^{-1}
4	8.03×10^{-9}	46.54	5.13×10^{-2}
5	3.667×10^{-8}	57.05	1.377×10^{-2}
6	3.46×10^{-5}	1.855	4.744×10^{-7}
7	5.518×10^{-6}	5.523	8.86×10^{-6}
8	9.045×10^{-7}	16.4	1.604×10^{-4}
9	1.522×10^{-7}	46.66	2.712×10^{-3}

5. Conclusions

A simple algorithm has been devized to optimize the equivalent network for a dielectric characterized by a distribution of relaxation times. The proposed procedure takes into account the distribution function, and its derivative, in defining the relaxation time interval for each network branch. The optimization has been applied on the dispersion data perfluoropolyether dielectric yielding more than 50% reduction in branches in addition to an improved accuracy for the network.

In principle, the methodology is applicable to dispersion relations featuring multiple arcs and in particular those with weak overlapping, such as in ZnO varistors [4, 7]. This may be readily accessible by treating each arc separately according to the algorithm while taking into account the arc's weighting factor [7]. Evidently, more efforts may be required in standardizing the procedure for arcs with strong overlapping [4], which is likely to be the case in polymeric and composite materials.

Acknowledgement

The author would like to acknowledge the financial support granted towards this work from the council of scientific research at Yarmouk University, Jordan.

References

1. S. N. AL-REFAIE, *Solid-State Electron.* **37** (1994) 1371.
2. H. S. B. ELAYYAN and S. N. AL-REFAIE, *J. Mater. Sci.* **31** (1996) 1199.
3. S. N. AL-REFAIE, *Appl. Phys. A* **57** (1993) 279.
4. *Idem.*, *ibid.* **62** (1996) 493.
5. *Idem.*, *ibid.* **52** (1991) 234.
6. M. GRAZIA GIRI, M. CARLA, C. M. C. GAMBI, D. SENATRA, A. CHITTOFRATI and A. SANGUINETI, *Meas. Sci. Technol.* **4** (1993) 627.
7. S. N. AL-REFAIE and H. S. B. ELAYYAN, *J. Mater. Sci. Lett.* **11** (1992) 988.

Received 31 October 1996
and accepted 9 May 1997